IEEE Photonics Journal
An IEEE Photonics Society Publication
Open Access

IEEE Xplore® Digital Library
http://ieeexplore.ieee.org/Xplore

Phase-Aligned Physical-Layer Network Coding in Visible Light Communications

Xun Guan[1] and Qing Yang[2], *Member, IEEE*, Taotao Wang[2], *Member, IEEE*, and Calvin Chun-Kit Chan[3], *Member, IEEE*

[1]The Center for Optics, Photonics, and Lasers (COPL), Université Laval, Québec, QC, Canada
[2]The College of Information Engineering, Shenzhen University, Shenzhen, Guangdong, China
[3]The Department of Information Engineering, The Chinese University of Hong Kong, Shatin, N.T., Hong Kong

DOI: 10.1109/JPHOT.2009.XXXXXXX
1943-0655/$25.00 ©2009 IEEE

Manuscript submitted on 27 December 2018.

Abstract: Deploying relay nodes in visible light communication (VLC) relieves the requirement of line-of-sight (LoS) transmission thus extends the service coverage of VLC systems. In this work, we propose to employ physical-layer network coding (PNC) in the VLC system to increase its throughput by boosting the data transmission at the relay node. We design a unified PNC-VLC framework that includes both the physical-layer signal processing algorithm and the medium access control method. To further improve the feasibility, we propose a novel phase-aligning method to counter the phase offset among nodes in practical VLC systems. Experimental results show a throughput improvement of 88.23% by employing the PNC-VLC framework, and the link budget is reduced by 4 dB at a bit error rate of 3.8×10^{-3} by using the phase-aligning method.

Index Terms: Visible light communication (VLC), physical-layer network coding (PNC),phase alignment, power ratio.

1. Introduction

Visible light communication (VLC) [1]–[8] is an attractive optical wireless communication technology exploiting the information transmission potential of widely deployed commercial light-emitted diodes (LEDs) or visible laser diodes (LDs), in addition to the basic function of illumination. With its high throughput, low cost, ease of integration with existing lighting facilities, and high security, VLC is expected to be a promising complement of the current wireless communication systems, as well as an enabling technology for the Internet of Things (IoT) [9], [10].

The practical application and deployment of VLC, however, are hindered by two limitations. First, the LEDs' and LDs' transmission range is short, subject to its limited brightness, fast decay, and the divergence of light [9]. Second, VLC mostly requires line-of-sight (LoS) transmission or the received light signal may be very weak. Similar drawbacks are also found in millimeter-wave wireless communication technologies [11]. Nevertheless, they could be alleviated by means of adopting relays in the system [12]. The relay technology can effectively extend the coverage of VLC and bypass the LoS obstacles, thus enables the deployment of large-scale VLC networks. Two-way relay network, which supports bi-directional information exchange, via the relay node, is the most common relay pattern. For a two-way relay-assisted connection in VLC, the throughput is bottlenecked at the relay node. In this paper, we propose a physical-layer network coded visible

Digital Object Identifier 10.1109/JPHOT.2019.2904954

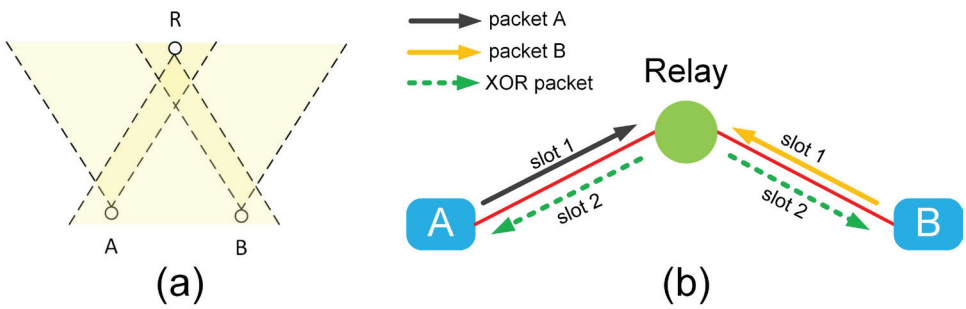

Fig. 1. (a) A typical two-way relay channel in visible light communication. Node A and node B are within node R's coverage, thus they can communicate with R respectively; however, node A and node B cannot communicate directly because there is no LoS path between them. Therefore the information exchange between A and B must be relayed by R. (b) Two end nodes exchange a pair of packets via the relay node in the visible light communication network using physical-layer network coding.

light communication (PNC-VLC) framework which can effectively boost the throughput of the VLC networks.

The idea of physical-layer network coding (PNC), first proposed in 2006 [13], is to exploit network coding [14] at the physical layer. As a novel interference-exploiting scheme to improve the overall throughput, PNC has been successfully introduced to different application scenarios, such as wireless communication [15], powerline communication [16], direct detected optical communication [17], [23], and coherent optical communication [18]. In the simplest PNC-VLC setup, two nodes, each equipped with an LD and a photodiode (PD), exchange information, via a relay, in a two-way relay network (TWRN). The two nodes first transmit their messages simultaneously to the relay where the overlapped signals are used to form a network-coded message, before being further broadcasted to the two nodes. Each of the two nodes retrieves the message from the other node based on the network-coded message and the knowledge of its own message [19]–[21].

Our PNC-VLC is the first work that employs PNC to boost the throughput of visible light communication networks. We have designed both the medium access control (MAC) and the physical (PHY) layers of the proposed PNC-VLC system. In particular, we have experimentally demonstrated a quadrature phase-shift keying (QPSK) modulated PNC-VLC system. To reduce the signal-to-noise ratio penalty, we have designed a phase-aligning (PA) method to further improve the performance and enhance the feasibility of the PNC-VLC system.

The rest of the paper is organized as follows. Section 2 describes the system model of the PNC-VLC system. Section 3 illustrates our PNC decoding algorithm used by the relay and analyses the proposed phase-aligning scheme for our PNC-VLC system. Section 4 shows our experimental results and analyses. Finally, Section 5 summarizes the paper.

2. System Model

In this section, we will discuss the principle of PNC and its application to our VLC system. We will further present our proposed beacon-triggered MAC protocol for the PNC-VLC system.

2.1. Physical-Layer Network Coding Principle in Visible Light Communication

Fig. 1(a) shows a two-way VLC system with a relay node. The two end nodes (node A and node B) exchange a pair of packets with each other, via a relay node (node R). Each of the nodes A, B, and R is equipped with an LD as the transmitter and a photodiode (PD) as the receiver. The communication between nodes A and B must be relayed by node R, due to lack of LoS path between them.

The system model can be abstracted to a widely recognized PNC model, as illustrated in Fig. 1(b), in which nodes A and B exchange a pair of packets PA and PB, respectively, through

the relay node R. Conventionally, nodes A and B need four time slots to exchange their respective packets PA and PB, via node R. However, as depicted in Fig. 1(b), the PNC scheme allows simultaneous transmission of the two packets, PA and PB, and the relay node R decodes the received packets into a logic exclusive OR (XOR) packets, using the PNC decoding algorithm, before broadcasting it to both nodes A and B. Each of the two end nodes then retrieves the packet sent from the other node, based on the received XOR packet and the knowledge of its own packet sent. As a result, the PNC-VLC system reduces the required number of time slots to two only in such packet exchange between two nodes, thus improves the net throughput by 100%, compared with conventional relay method.

2.2. Physical-Layer Design of PNC-VLC

The VLC channel is similar to the wireless communication channel which suffers from frequency selective fading [7], [24]. To enable reliable communication, we design the physical-layer (PHY) of our PNC-VLC system, based on the widely used orthogonal frequency division multiplexing (OFDM) modulation technique, so as to adapt to the frequency-selective channel. We adopt OFDM modulation with intensity modulation. The packet exchange in our PNC-VLC system consists of two phases: multiple access phase and broadcast phase. Each phase takes one time slot. In the first time slot, nodes A and B modulate their respective source packets into OFDM signals. We denote them by two binary sequences

$$U^i = \left(u_1^i, u_2^i, \cdots, u_L^i\right),\ i \in \{A, B\}, \tag{1}$$

where L is the length of the binary sequence and u_l^i is the lth input bit of the end node i's source packet. Next, U^A and U^B are fed into their respective OFDM modulator to produce the two sequences of baseband complex symbols. We focus on quadrature phase-shift keying (QPSK) mapping in this paper, but our framework can be easily extended to other higher order constellations such as 16QAM. Let $\mathbf{X}^i$ denote frequency-domain signals after QPSK mapping of node U^i, and let $X_{k,n}^i$ denote the complex sample of $\mathbf{X}^i$ on the kth subcarrier and nth OFDM symbol. Hence the transmitted frequency-domain signals are

$$\mathbf{X}^i = \begin{bmatrix} X_{1,1}^i & X_{1,2}^i & \cdots & X_{1,N}^i \\ X_{2,1}^i & \ddots & & \\ \vdots & & \ddots & \vdots \\ X_{K,1}^i & & \cdots & X_{K,N}^i \end{bmatrix},\ i \in \{A, B\}, \tag{2}$$

where K is the number of subcarriers and N is the number of OFDM symbols.

After the QPSK mapping, we perform inverse fast Fourier transform (IFFT) on $\mathbf{X}^i$ to produce the time-domain OFDM symbols and append the cyclic prefix (CP) to each OFDM symbol. These symbols are then intensity-modulated and transmitted to the relay node, via the LDs.

Upon receiving the time-domain overlapped signal from nodes A and B, the relay node removes the CP and performs fast Fourier transform (FFT) to obtain the frequency-domain signal $\mathbf{Y}^R$. The relay node then demaps the frequency-domain signal to produce the XOR source packet U^R, which is an estimate of $U^A \oplus U^B$. This demapping process will be elaborated in Section 3. In the second time slot, the relay node broadcasts U^R to both the destined end nodes, via the conventional VLC transmission.

2.3. PNC-VLC Frame Format and Medium Access Control Method

In this work, we focus on our MAC design for the two-way relay communication pattern, as illustrated in Fig. 2(c) and leave the investigation of multiple-node PNC for future work. The PNC-VLC frame includes the training sequence (TS) and the payload. The TS is used by the receiver to estimate the channel state information (CSI) and perform packet detection and synchronization. We let nodes A and B employ orthogonal TS, allowing the relay node to

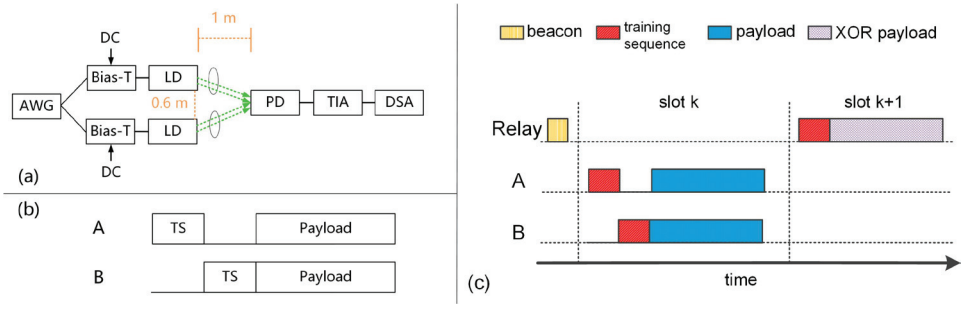

Fig. 2. (a) Visible light communication hardware platform setup. AWG: arbitrary waveform generator; LD: laser diode; PD: photodiode; TIA: trans-impedance amplifier; DSA: digital serial analyzer. (b) The frame format used by end node A and B. TS: training sequence. (c) The media access control (MAC) procedure of the PNC-VLC.

estimate the CSI between itself and nodes A or B, separately. As depicted in Fig. 2(c), we insert a sequence of zeros after node A's TS and also before node B's TS, therefore the TSs of both nodes A and B are non-overlapping (or orthogonal).

The goal of our MAC protocol design is to enable the two end nodes to transmit simultaneously to the relay node in the first time slot. We let the relay node broadcast a beacon signal to trigger the simultaneous transmission at the end nodes, as depicted in Fig. 2(c). Upon receiving the beacon signal, the end nodes A and B transmit their packets simultaneously in the next time slot. Note that in the following time slot, the beacon can be piggy-backed with the broadcasted packet. The two packets sent from nodes A and B may not arrive at the relay node precisely at the same moment. Such possible imperfect time synchronization can be attributed to the different processing delay and transmission delay for nodes A and B. This time asynchrony, however, can be alleviated by OFDM modulation, as long as it is within the duration of the CP.

Upon receiving the overlapped packet, the relay node first estimates the CSIs of both nodes A and B, using the orthogonal training sequences, respectively. It then decodes the overlapped payload into the XOR payload, using the PNC decoding technique to be explained in the next section. In the second time slot, the relay node broadcasts the XOR payload $U^R = U^A \oplus U^B$ to both the two destined end nodes, via conventional VLC transmission. After receiving the broadcasted packet U^R, node A retrieves the source packet U^B from node B by performing the logic XOR operation on U^R with its own packet U^A. Using a similar procedure, node B can also retrieve node A's source packet U^A.

The discussion of the PNC-VLC above is only limited to the simple two-way relay case. However, the application of PNC-VLC, with a slight modification of the MAC layer, can be scaled up to larger networks. First, we consider the multi-way relay network in which multiple end nodes exchange packets via the relay node in the center [22]. In this case, the the PHY layer still applies and the relay picks up two end nodes to form a PNC relay setup in each time slot. Second, our PNC-VLC network can be extended to a multi-hop chain network when more relay nodes join the network. In the multi-hop chain network, the PNC-VLC can be applied to each hop of the relay chain, thus to improve the overall throughput. Both of the two methods scale the PNC-VLC network to more general networks, with only slight modification of the MAC layer and the PHY layer remaining the same as discussed in this section. Due to the scope of this paper, we will limit our analysis to the basic two-way relay setup of PNC-VLC in the remaining parts.

3. Phase-Aligned Visible Light Communication for Physical-Layer Network Coding

In this section, we will first explain the PNC demapping algorithm used at the relay node to map the received overlapped packet into the XOR packet. Then we present a new phase-align method

for VLC-PNC to improve its BER performance under non-ideal channel condition and also analyze the performance of this method.

3.1. VLC-PNC Signal Processing at the Relay Node

In the first time slot of the PNC-VLC system, the relay's received signal has a singular constellation map which is the overlapping of the signal constellation from nodes A and B. However, the overlapped constellation, due to the phase difference between the channel coefficients of the two end nodes, may not have the optimal signal constellation point layout, and thus sometimes even leads to possible decoding failure [20]. In this section, we describe our phase-aligning method for the PNC-VLC system to align the signal constellations at the end nodes A and B, so that their overlapped constellation at the relay node can be optimal and thus achieves good decoding performance at the respective receiving end nodes.

At the relay node, the received overlapped packet is first down-converted to the baseband. Based on the orthogonal training sequence of the OFDM signal, the relay node can estimate the CSI between itself and the two end nodes. After removing the CP from each OFDM symbol in the payload part, the relay node performs FFT on the overlapped symbols and obtains the frequency-domain baseband signal $\mathbf{Y}^R$. Let $Y^R_{k,n}$ denotes the nth sample on the kth subcarrier of $\mathbf{Y}^R$, hence,

$$Y^R_{k,n} = h^A_k X^A_{k,n} + h^B_k X^B_{k,n} + w^R_{k,n}, \tag{3}$$

where $X^i_{k,n}$ denotes the nth sample on the kth subcarrier of $\mathbf{X}^i$, which is the transmitted signal (in frequency domain) from node i, while the channel coefficients of the kth subcarrier channels from nodes A and B to the relay node are represented by h^A_k and h^B_k, respectively, both of which are complex numbers. The relative phase difference between h^A_k and h^B_k is denoted by $\phi_k = \angle\left(h^B_k/h^A_k\right)$ on the kth subcarrier, and $w^R_{k,n}$ is the Gaussian noise on the kth subcarrier with variance σ^2.

Upon receiving the overlapped packet, the XOR mapping module at the relay node first compute the likelihood of the signals, $X^A_{k,n}$ and $X^B_{k,n}$,

$$\Pr\left(Y^R_{k,n}\middle|\, X^A_{k,n}, X^B_{k,n}\right) = \frac{1}{\sqrt{2\pi\sigma^2}} \exp\left\{-\frac{\left|Y^R_{k,n} - h^A_k X^A_{k,n} - h^B_k X^B_{k,n}\right|^2}{2\sigma^2}\right\}. \tag{4}$$

The relay node then calculates the likelihood of the XORed bit $\mathbf{X}^R_{k,n}$, denoted by $\Pr\left(Y^R_{k,n}\middle|\, X^R_{k,n}\right)$, based on (4), and decodes the XOR output by maximizing the likelihood function,

$$\begin{aligned}\hat{X}^R_{k,n} &= \arg\max_{X^R_{k,n}} \Pr\left(Y^R_{k,n}\middle|\, X^R_{k,n}\right) \\ &= \arg\max_{X^R_{k,n}} \sum_{X^A_{k,n}, X^B_{k,n}: X^A_{k,n} \oplus X^B_{k,n} = X^R_{k,n}} \Pr\left(Y^R_{k,n}\middle|\, X^R_{k,n}\right),\end{aligned} \tag{5}$$

where $\hat{X}^R_{k,n}$ is the decoding output of the XOR mapping algorithm. After the XOR mapping, the relay node obtains $\mathbf{X}^R = \mathbf{X}^A \oplus \mathbf{X}^B$, which is the bit-by-bit logic XOR of packet A and packet B.

3.2. BER Performance Analysis

In the PNC-VLC system, we perform per-subcarrier PNC decoding and the decoding algorithm has been expressed in the previous section. In this decoding method, we classify the points of the overlapped signal constellation (in total 16 points) into four groups based on their XOR values. Therefore, the received signal constellation plane is partitioned into four regions. When a signal point falls into one of these regions, it is decoded into the XOR value corresponding to that region. Let $X^{XOR}_{k,n}$ denotes the center point of the signal constellation points having the same XOR value

in one particular region, (5) can be expressed as

$$\hat{X}_{k,n}^{R} = \arg\max_{X_{k,n}^{R}} \Pr\left(Y_{k,n}^{R} \middle| X_{k,n}^{XOR}\right) = \arg\max_{X_{k,n}^{R}} \frac{1}{\sqrt{2\pi\sigma^2}} \exp\left\{-\frac{\left|Y_{k,n}^{R} - X_{k,n}^{XOR}\right|^2}{2\sigma^2}\right\}. \tag{6}$$

Therefore, by the theorem of union bound, the BER of this decoding algorithm is bounded by

$$P_e \leq (M-1)\, Q\left(\frac{d_{\min}}{\sqrt{2N_0}}\right), \tag{7}$$

where M is the number of the signal constellation points of the composite overlapped signal ($M = 16$ here); N_0 is the single-sided power spectrum density of the noise; $d_{\min}$ is the minimum distance between any pair of constellation points in one particular region in the signal constellation. In the PNC-VLC system, in which QPSK format is used at both end nodes, the minimum distance is

$$d_{\min} = \sqrt{2}\left|h_k^A - (1+j)h_k^B\right| = \left|1 - \frac{1+j}{r_k e^{j\varphi_k}}\right|, \quad 0 < \varphi \leq \frac{\pi}{4}, \tag{8}$$

where $r_k = \left|h_k^A / h_k^B\right|$ is defined as the signal power ratio (PR) of that from node A to that from node B. And $\phi_k = \angle\left(h_k^A / h_k^B\right)$ is the phase offset between the channel coefficients at the two end nodes. As the signal constellation here is centro-symmetric, we have considered the range of $\varphi \in (0, \frac{\pi}{4}]$ only. Here we assume perfect power control such that the power ratio $r_k = 1$ on all subcarriers (imperfect power control case will be discussed in Section 4.2). The maximum of $d_{\min}$ is achieved when φ is zeros, meaning that best BER performance is achieved when the signal constellations from nodes A and B are aligned.

To achieve optimal BER performance of the PNC-VLC system, we have designed a method to align the phases of the signal constellations from the two end nodes, based on the channel state information (CSI) measured at the relay node. As discussed in Section 2.3, the orthogonal TS design allows the relay to estimate the CSIs (h_k^A and h_k^B) between itself and the nodes A or B individually. Then the relay feedbacks the measured CSIs to both nodes A and B, via the broadcast beacon signal. Upon receiving the CSI, node A extracts the phase offset of the kth subcarrier with respect to the relay, denoted by $\angle h_k^A$, and multiplies its transmitting signal on the kth subcarrier by $e^{-j\angle h_k^A}$. Node B applies the same method on its transmitting signal with $e^{-j\angle h_k^B}$. As a result, the transmitted signal of nodes A and B will arrive at the relay node with zero phase offset, thus they are phase aligned.

In the second time slot of the PNC-VLC system, the relay node broadcasts the XOR packet $\mathbf{X}^R$ to both nodes A and B, via the conventional point-to-point VLC transmission. After receiving the XOR packet, node A can simply retrieve the packet from node B by performing logic XOR to $\mathbf{X}^R$ with its own transmitted packet $\mathbf{X}^A$, that is

$$\mathbf{X}^A \oplus \mathbf{X}^R = \mathbf{X}^A \oplus \left(\mathbf{X}^A \oplus \mathbf{X}^B\right) = \mathbf{X}^B. \tag{9}$$

Similarly, node B can also retrieve the packet sent from node A by performing logic XOR to $\mathbf{X}^R$ with its own transmitted packet $\mathbf{X}^B$.

4. Experiments and Discussion

4.1. Experimental Setup

Fig. 2(a) depicts our hardware platform for the PNC-VLC system. We generated the transmitted data samples offline using MATLAB, and they were fed to an arbitrary waveform generator (AWG, Tektronix 7122C), which outputs two electrical signals for nodes A and B, individually. Biased by the two separate bias-tees (Bias-T), the electrical signals were fed to two green visible laser diodes (Osram PL520 and its 3dB bandwidth is 150MHz) so as to generate the respective modulated optical signals. The relay node, equipped with a photodiode (Hamamatsu S10784 and its cutoff

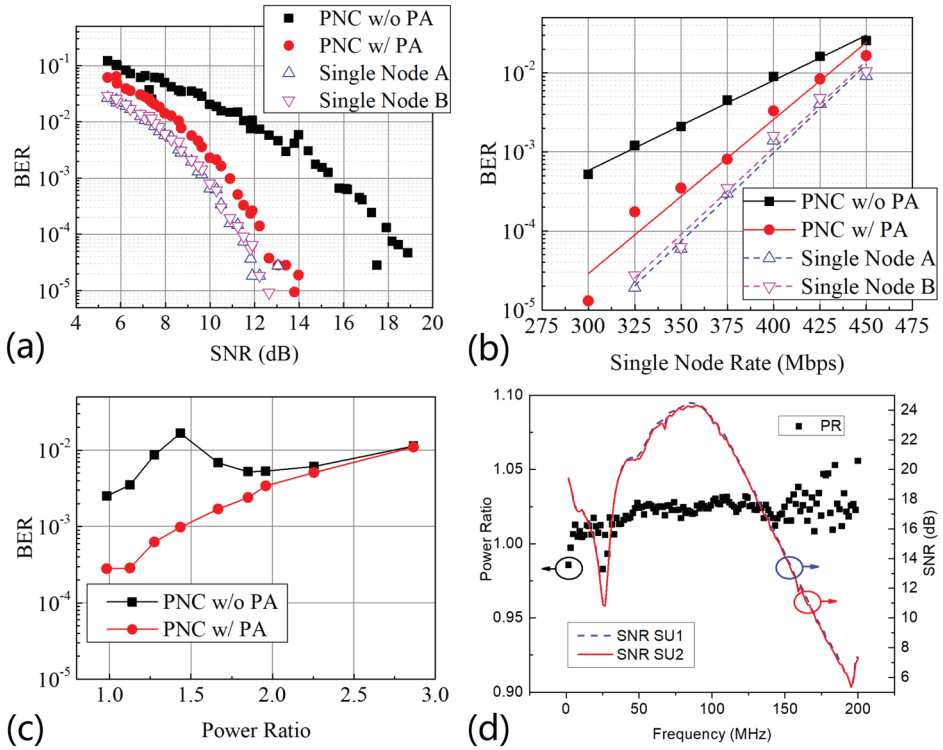

Fig. 3. Experiment results summary (a) BER vs SNR; (b) BER vs. single user rate; (c) BER vs. power ratio. (d) Signal to noise ratio and power ratio of two nodes. SNR: signal to noise ratio. PR: power ratio between the two users.

frequency is 250MHz), was placed one meter away from both LDs. We placed two sets of lenses in front of the LDs to focus the two light beams onto the relay node's PD.

At the relay node, the received visible light signal was converted into an electrical signal, via the PD, which was then amplified by a trans-impedance amplifier (TIA) before being sampled by a digital signal analyzer (DSA, Tektronix 72004B). The digital samples were then offline-processed by our PNC decoding algorithm (described in Section 3) in MATLAB. As the phase-aligned PNC required the two end nodes' CSIs for phase alignment, we appended the training sequence (TS) to each frame for channel estimation. As the CSIs of nodes A and B should be estimated individually, their respective TS should not overlap at the relay node. Hence, we designed the frame structure, as shown in Fig. 2(b), such that the TS of nodes A and B were orthogonal, thus their respective CSIs can be estimated.

The experimental procedure of the phase-aligned PNC consists of two steps. In the first step, the two end nodes transmit empty frames, which contained only the TS part, to the relay node for CSI estimation. The relay node then reported the measured CSIs to the end nodes, where the received CSI was used to align the phase of the payload signals. In the second step, the end nodes transmitted the phase-aligned signals to the relay node. We adopted 256-point FFT in the OFDM modulation and the cyclic prefix length is 16. Each OFDM frame consists of 8 symbols of training sequences and 240 symbols of payload. To evaluate the performance of this system, the BER was measured at the relay node by counting the number of erroneous bits in 200 frames, each composed of 240 payload OFDM symbols.

4.2. Results and Discussions

In the first experiment, we measured the frequency response of the visible light channel in our hardware platform and verified the viability of our channel estimation and power control methods.

We first adjusted the per-subcarrier power ratio (PR) between the two nodes to 1. The sampling rate of AWG was set to 400 MSa/s. The training sequences were used to estimate the frequency responses of the two end nodes, respectively. Fig. 3(d) shows the SNRs of the received signals and also the PRs of the two nodes at different subcarrier frequencies. The measured VLC channel showed strong frequency selectivity. The SNR initially dropped to 10 dB at about 28 MHz and then increased drastically to its peak value 24 dB at 100 MHz. It started to drop when the frequency exceeds 100 MHz.

In Fig. 3(a), the BER performance of the phase-aligned scheme (PA-PNC) was compared to the non-phase-aligned scheme (non-PA-PNC), benchmarked with a conventional relay scheme, which only involved the transmission from an end node to the relay node in a point-to-point transmission. It is shown that the PA-PNC only incurred about 1 dB SNR penalty at the BER of 3.8×10^{-3}, which was moderate considering the great improvement achieved by PNC. By contrast, the non-PA-PNC showed a remarkable SNR gap of 4 dB compared to the PA-PNC at a BER of 3.8×10^{-3}. Therefore, using the phase-aligned scheme reduces the total link budget by 4 dB at the 7% FEC limit.

Fig. 3(b) depicts the measured BERs of different schemes with regard to different single user transmission rates, which can be controlled by adjusting the sampling rate of the AWG. As shown in the figure, the system BERs of all transmission schemes increased as the end nodes? transmission rates increased. This could be attributed to the wider signal bandwidths at higher transmission rates and thus it was more vulnerable to the frequency-selective channel. Below a BER of 3.8×10^{-3}, the PA-PNC scheme achieved a maximum rate of 400 Mbps, while the non-PNC scheme could transmit at 425 Mbps at most. As the transmission time of the PNC scheme was only half of the non-PNC scheme, the throughput improvement achieved by adopting PA-PNC was about 88.23%. Besides, the PA-PNC scheme showed a 50 Mbps throughput improvement compared to the non-PA-PNC scheme.

In order to investigate the impact of the power ratio between the two nodes on our PA-PNC system, we fixed the sampling rate of AWG at 350 MSa/s and changed the PR of the two nodes from one to three. Fig. 3(c) shows the measured BERs with regard to the values of PR.

Following our analysis in (7) and (8), without phase-alignment (i.e., the phase offset φ_k is randomly distributed on $(0, \pi/4]$), the BER can be calculated by integrating (7) with respect to φ_k,

$$P_e \leq \int_0^{\pi/4} \frac{4}{\pi} (M-1)\, Q\left(\frac{\left|1 - \frac{1+j}{r_k e^{j\varphi_k}}\right|}{\sqrt{2N_0}} \right) \mathrm{d}\varphi_k. \tag{10}$$

It was found that the BER reached its maximum value when the PR was 1.4, by numerical analysis, which matched with our experimental results, as shown in Fig. 3(c). The results also showed that PA-PNC outperformed non-PA-PNC under different power ratios. The BER of PA-PNC increased smoothly as the PR increased. Therefore, power control could be applied to a PNC-VLC system for a better BER performance.

5. Summary

We presented a physical-layer network coded visible light communication (PNC-VLC) framework to boost the throughput of the VLC relay system. To further improve the feasibility of PNC-VLC, we proposed a novel phase alignment scheme to counter the phase offset between the end nodes thus improve the BER performance of PNC-VLC in practice. Both theoretical analysis and experiments have been conducted to evaluate the phase-aligned PNC in VLC systems. Experimental results showed that an 88.23% improvement in throughput was achieved by the adoption of PNC, compared to the non-PNC scheme. Besides, the effect of the power ratios was also experimentally studied and the results agreed with our theoretical analysis. In addition, the phase alignment method reduced the link budget by 4 dB to achieve a BER of 3.8×10^{-3}, which further enhanced the practicality of the proposed PNC-VLC framework.

Acknowledgements

This work was partially supported by a research grant from Hong Kong Research Grants Council (GRF Project No. 14200614). It is also partially supported in part by the National Natural Science Foundation of China under Grant 61701311, and in part by the Natural Science Foundation of Guangdong Province, China, under Grant 2017A030310334, and in part by the Shenzhen NSF project under grant JCYJ20170818095107583.

References

[1] D. O'Brien, G. Parry, and P. Stavrinou, "Optical hotspots speed up wireless communication," *Nat. Photon.*, vol. 1, no. 5, pp. 245–247, 2007.
[2] Q. Wang, Z. Wang, and L. Dai, "Multiuser MIMO-OFDM for visible light communications," *IEEE Photon. J.*, vol. 7, no. 6, pp. 1–11, 2015.
[3] Y. Hong, J. Chen, Z. Wang, and C. Yu, "Performance of a precoding MIMO system for decentralized multiuser indoor visible light communications," *IEEE Photon. J.* , vol. 5, no. 4, pp. 7800211–7800211, 2013.
[4] L.Y. Wei, C.W. Hsu, C.W. Chow, and C.H. Yeh, "20.231 Gbit/s tricolor red/green/blue laser diode based bidirectional signal remodulation visible-light communication system," *Photonics Research*, vol. 6, no. 5, pp. 422–426, 2018.
[5] T.C. Wu, Y.C. Chi, H.Y. Wang, C.T. Tsai, Y.F. Huang, and G.R. Lin, "Tricolor R/G/B laser diode based eye-safe white lighting communication beyond 8 Gbit/s," *Scientific reports*, vol. 7, no. 1, pp. 11, 2017.
[6] C.H. Yeh, L.Y. Wei, and C.W. Chow, "Using a single VCSEL source employing OFDM downstream signal and remodulated OOK upstream signal for bi-directional visible light communications," *Scientific reports*, vol. 7, no. 1, pp. 15846, 2017.
[7] N. Chi, *Led-Based Visible Light Communications*, Berlin, Germany: Springer-Verlag GmbH, 2018.
[8] S. Watson, M. Tan, S. P. Najda, P. Perlin, M. Leszczynski, G. Targowski, S. Grzanka, and A. E. Kelly, "Visible light communications using a directly modulated 422nm GaN laser diode," *Optics Letters*, vol. 38, no. 19, pp. 3792–3794, 2013.
[9] T. Komine, and M. Nakagawa, "Fundamental analysis for visible-light communication system using LED lights," *IEEE Trans. Consum. Electron.*, vol. 50, no. 1, pp. 100–107, 2004.
[10] Y. Wang, N. Chi, Y. Wang, L. Tao, and J. Shi, "Network architecture of a high-speed visible light communication local area network," *IEEE Photon. Technol. Lett.*, vol. 27, no. 2, pp. 197–200, 2015.
[11] K. Cui, G. Chen, Z. Xu, and R. D. Roberts, "Line-of-sight visible light communication system design and demonstration," in *7th IEEE International Symposium on Communication Systems Networks and Digital Signal Processing*, pp. 621–625, 2010.
[12] R. C. Kizilirmak, R. Caglar, and M. Uysal, "Relay-assisted OFDM transmission for indoor visible light communication," in *IEEE International Black Sea Conference on Communications and Networking*, pp. 11–15, 2014.
[13] S. Zhang, S. C. Liew, and P. P. Lam, "Hot topic: physical-layer network coding," in *Proceedings of the 12th annual international conference on Mobile computing and networking (ACM Mobicom)*, pp. 358–365, 2006.
[14] S. Y. R. Li, Raymond W. Yeung, and Ning Cai, "Linear network coding," *IEEE Trans. Inf. Theory*, vol. 49, no. 2, pp. 371–387, 2003.
[15] L. Lu, T. Wang, S. C. Liew, and S. Zhang, "Implementation of physical-layer network coding," *Physical Communication*, vol. 6, pp. 74–87, 2013.
[16] Q. Yang, H. Wang, T. Wang, L. You, L. Lu, and S. C. Liew, "Powerline-PNC: boosting throughput of powerline networks with physical-layer network coding", in *IEEE International Conference on Smart Grid Communications*, pp. 103–108, 2015.
[17] Z. Liu, M. Li, L. Lu, C. K. Chan, S. C. Liew, and L. K. Chen, "Optical physical-layer network coding," *IEEE Photon. Technol. Lett.*, vol. 24, no. 16, pp. 1424–1427, 2012.
[18] M. Li, Y. Wu, L. K. Chen, and S. C. Liew, "Common-channel optical physical-layer network coding," *IEEE Photon. Technol. Lett.*, vol. 26, no. 13, pp. 1340–1342, 2014.
[19] S. C. Liew, L. Lu, and S. Zhang, "A primer on physical-layer network coding," in *Synthesis Lectures on Communication Networks*, vol. 8, no. 1, pp. 1–218, 2015.
[20] L. Lu, and S. C. Liew, "Asynchronous physical-layer network coding," *IEEE Trans. Wireless Commun.*, vol. 11, no. 2, pp. 819–831, 2012.
[21] Q. Yang, S. C. Liew, "Asynchronous convolutional-coded physical-layer network coding," *IEEE Trans. Wireless Commun.*, vol. 14, no. 3, pp. 1380–1395, 2015.
[22] J. He, S. Liew, "Building blocks of physical-layer network coding," *IEEE Trans. Wireless Commun.*, vol. 14, no. 5, pp. 2711–2728, 2015.
[23] C. Mitsolidou, C. Vagionas, K. Ramantas, D. Tsiokos, A. Miliou, and N. Pleros, "Digital optical physical-layer network coding for mm-wave radio-over-fiber signals in fiber-wireless networks," *J. Lightw. Technol.*, vol. 34, no. 20, pp. 4765–4771, 2016.
[24] F. Miramirkhani and M. Uysal, "Channel modeling and characterization for visible light communications," *IEEE Photon. J.*, vol. 7, no. 6, pp. 1–16, 2015.